Supplementary Materials for

The Mammalian MAPK/ERK Pathway Exhibits Properties of a Negative Feedback Amplifier

Oliver E. Sturm, Richard Orton, Joan Grindlay, Marc Birtwistle, Vladislav Vyshemirsky, David Gilbert, Muffy Calder, Andrew Pitt, Boris Kholodenko, Walter Kolch*

*To whom correspondence should be addressed. E-mail: walter.kolch@ucd.ie

This PDF file includes:

Section 1. Models and modeling.
Section 2. Model parameters.
Section 3. SBML files of the models.
References
Fig. S1. Absolute concentrations of Raf-1, MEK, and ERK in COS1 and NIH 3T3 cells.
Fig. S2. Schematic topologies of the models used.
Fig. S3. Schematic of Raf-1 and the Raf-1 mutants used to probe the NFA hypothesis.
Fig. S4. Expression of Flag-tagged Raf-1 and the Raf6A mutant.
Fig. S5. The effects of U0126 on steady-state ppERK abundance with protein concentrations of COS1 cells.
Fig. S6. The NFA effect also stabilizes non–steady-state dynamic systems.
Fig. S7. Dose-dependent ERK activation by different stimuli.
Fig. S8. B-Raf kinase activity is not feedback-inhibited by ERK.

Other Supplementary Material for this manuscript includes the following:
(available at www.sciencesignaling.org/cgi/content/full/3/153/ra90/DC1)

Tables S1 to S3. Model parameters (Microsoft Excel format).
SBML files of the models (.xml format).

Supplementary Sections 1-3, References, and Figures

Section 1. Models and Modelling

The mathematical models were based on mass action models using ordinary differential equations. We constructed two computational models, Feedback Intact and Feedback Broken, to investigate the negative feedback amplifier (NFA) characteristics of the extracellular signal-regulated protein kinase (ERK) pathway. These computational models were based on the core ERK pathway of the Schoeberl *et al*. model *(1)* and, therefore, utilize ordinary differential equations (ODEs).

1.1: Feedback Intact Model and Amplifier Perturbation

The Feedback Intact model (fig. S2A) starts at the level of Ras, ends at the level of ERK, and includes a negative feedback loop from activated ERK to both active and inactive Raf-1 executed by direct inhibitory phosphorylation of Raf-1 by ERK *(2)*. Because activation of Ras is the key obligatory event for Raf-1 activation by different receptor tyrosine kinases *(3-5)*, we used Ras activity (measured by the abundance of RasGTP) as a surrogate for receptor activity in the model. This means that the Feedback Intact model is focussed on the core ERK pathway, which is essentially the NFA module of interest. A table of reactions, species, and kinetic parameters for the Feedback Intact model is presented in the Model_Intact (table S1).

We used the specific MEK Inhibitor U0126 *(6)* to perturb the amplifier module. U1026 was originally characterized as a noncompetitive or mixed inhibitor *(7)*. Detailed enzyme

kinetic studies showed that U0126 does not prevent the activating phosphorylation of MEK by Raf kinases, but blocks binding and phosphorylation of the ERK substrate *(8)*. Structural studies suggest that MEK inhibitors interact with the substrate-binding domain of MEK and may lock MEK in an inactive conformation *(9)*. Thus, in the model, U0126 is represented as allosteric inhibitor, which can bind to all forms of MEK and does not interfere with the activation of MEK by Raf or the deactivation of MEK by its phosphatase.

In theory, the Feedback Intact model should behave similarly to a NFA because it has a constant input, an amplifier module, a constant output, and negative feedback loops. Therefore, the system should resist the effects of a MEK inhibitor, such as U0126. We employed the following strategy to investigate the resistance of the system to U0126, and, therefore, the NFA characteristics of the ERK pathway. Initially, the model has no U0126 present and is simulated for 3,600,000,000 seconds to reach a steady state, at which time the concentration of total activated ERK (ppERK) is obtained; total ppERK corresponds to all ppERK-containing species in the model and is used to compare to the Western blot laboratory data. Then, a new simulation is run, starting from the same initial conditions as before except in the presence of a low concentration of U0126; again, the model is simulated for 3,600,000,000 seconds to reach a steady state and the final concentration of total ppERK is obtained (simulations were examined to check that a steady state had been achieved). The initial concentration of U0126 is increased incrementally from 0, with a new simulation run at each increment stage and with the final concentration of total ppERK obtained for each simulation run. Plotting the initial concentration of U0126 against the final total concentration of ppERK for each simulation run reveals how the system responds to an increasing disturbance caused by U0126. We used the Scan function of the pathway simulation tool Gepasi (Mendes, 1999; www.gepasi.org) to create the graph. The Feedback Intact system i resists the effects of U0126 and maintain relatively high abundances of ppERK over a broad inhibitor concentration range (Fig. 3C).

1.2: Feedback Broken Model

The Feedback Broken model starts at BXB-ER and ends at ERK (fig. S2B). BXB-ER is an artificial fusion protein in which the kinase domain of Raf-1 is fused to the hormone-binding domain of the estrogen receptor *(10)*. The kinase activity of BXB-ER is independent of Ras activity and instead can be acutely regulated by the synthetic estrogen analog 4-hydroxy-tamoxifen (4HT) with activation kinetics similar to those of endogenous Raf-1 *(10, 11)* (Fig. 1F). BXB-ER lacks five of the six ERK feedback phosphorylation sites (fig. S3) and is completely resistant to negative feedback regulation by ERK (Fig. 1F). Therefore, this model lacks any negative feedback loops because activation of ERK through BXB-ER lacks both the ERK negative feedback loop to Raf-1 and to SOS and, thus, to Ras activation. The MEK inhibitor U0126 is incorporated in this model as described above. A table of reactions, species, and kinetic parameters for the Feedback Broken model is presented in the Broken_Model (table S2).

In theory, the Feedback Broken model should behave as a standard amplifier, and the system should be sensitive to even low concentrations of an amplifier inhibitor, such as U0126. The strategy to investigate the resistance of the system to U0126 was the same as described above for the Feedback Intact model. The results show that the Feedback Broken model is inhibited at low concentrations of U0126; whereas the Feedback Intact model is much more resistant to inhibition of the amplifier with ppERK abundance remaining relatively high over a broad concentration range.

1.3: Input Strengths Selection, Parameter Values, and Comparison Between Feedback Intact and Broken Models

To directly compare the relationship between input strength and dose response of the two models, they need to have comparable input strengths. The Feedback Broken model has BXB-ER as input, whereas the Feedback Intact model has RasGTP as input. For the purposes of comparing input dose and inhibition responses between the Feedback Broken and Feedback Intact models, we modified the Feedback Broken model with a pseudo-input S, which acts like RasGTP in the Intact model. We normalized the steady-state input and output relationships by the value of input (RasGTP or BXB-ER), which produced half-maximal ERK activation (Fig. M1). We also compared how the Feedback Broken and Intact models responded to input inhibition (Fig. M1). Although the Feedback Broken model resists input inhibition better than the Feedback Intact model at less than half-maximal inhibition, it displays catastrophic failure around half-maximal inhibition. This catastrophic failure is not observed with the Feedback Intact model, where ppERK abundances smoothly decline with increasing input inhibition. These results thus imply that the negative feedback provides robustness to input perturbations.

To determine appropriate input strengths to use in further simulations, we examined the input/output relationship of the model by scanning through the initial concentration of BXB-ER as input and monitoring the steady-state concentration of total ppERK as output. We selected an input strength of 4,000 BXB-ER molecules for the Feedback Broken model, because this was near the center of the input/output response curve (Fig. M1). For the Feedback Intact model, the input strength was consequently set to the concentration of RasGTP as input that yielded a total of approximately 4,000 activated Raf-1 molecules, which was comparable to the 4,000 BXB-ER molecules. Input/output analyses determined that this concentration was 5,350 RasGTP molecules (Fig. M1. Thus, the two models have equal input strengths, which have been normalized to the abundance of active Raf-1 molecules in the system. We also calibrated the Raf input experimentally by titrating 4HT to give BXB-ER activation strength and kinetics similar to those of EGF-activated endogenous Raf-1 (Fig. 1F). In the experiments with the Raf6A mutant, for the control we used cells that were transfected with wild-type Raf-1 expressed at similar abundance to that in cells expressing the Raf6A mutant (fig. S4). Thus, we can make reliable comparisons of the responses of the different (biological and computational) model systems to drug perturbations.

Our models are normalized to the Raf input strength, but other parameters were not adjusted to make the models equivalent. We explored how parameter changes affected

the responses to U1026 inhibition by comparing the Feedback Intact and Feedback Broken models (Fig. M2) in simulations in which each kinetic parameter, in both models (intact and broken), was sampled from a uniform distribution +/- 1 order of magnitude from its nominal value. We ran 1000 different steady-state simulations for every value of U0126, each with a different realization of the kinetic parameters. With 10 different U0126 concentrations, this corresponds to 10,000 parameter sets. The results show that even under these widely varying parameter conditions the shape of the response curves in both models stays essentially the same (fig. M2).

1.4: EGFR Inhibitor

Because the amplifier is located within the negative feedback loop, NFAs compensate for disturbances to the amplifier and, therefore, maintain relatively stable output strengths. However, NFAs do not compensate for disturbances to the input, because the input is located outside of the negative feedback loop. Applying this to the biological situation implies that drugs, like U0126, that target components embedded within the negative feedback loop will be less effective than drugs targeting components outside of the feedback amplifier module. An example of such a drug is the EGF receptor (EGFR) inhibitor 4557W, which binds to the EGFR and blocks its kinase activity *(12)*. Therefore, 4557W decreases the number of receptors that can activate the downstream ERK pathway and interferes with the input into the negative feedback amplifier, for which the system should be unable to compensate.

Because the Feedback Intact model starts at the level of RasGTP, rather than the EGFR itself, the effects of 4557W cannot be modelled directly. However, the effects of 4557W on the input into the NFA module can be investigated within a qualitative, core model, where the effect of decreasing the number of activated EGFR is modelled as a decrease in the initial RasGTP abundance. Technically, this was accomplished with the Scan function of Gepasi.

1.5: Sensitivity Analysis

Sensitivity analysis is a commonly used approach to study the response of system variables to changes in parameter values and can therefore be used to identify the key reactions and species in a model *(13)*. Furthermore, sensitivity analysis can also be used to assess the robustness of a model. Sensitivity analysis works by varying a parameter value by a small amount and analyzing what effect this has on a specific system variable, for example, the steady-state concentration of total ppERK. A small change to a key parameter value is likely to have a large effect on the system variable. It is important to note that different parameters can have widely different sensitivities, and the sensitivity of a specific parameter can also vary depending on which system variable is considered. The sensitivity coefficient (SC) of a specific parameter P with respect to a specific system variable V can be calculated using Equation 1; δV represents the change in the system variable V due to the change in the parameter P (δP).

$$SC_P^V = \frac{\delta V / V}{\delta P / P}$$

Equation 1. *Sensitivity Coefficient (SC) equation of parameter P with respect to system variable V.*

We performed sensitivity analysis to compare how robust the Feedback Intact and Feedback Broken models were in the absence of inhibitors (Fig. 2B). We individually varied every kinetic rate constant +10% in each of the two models and monitored the effect of each variation on total steady state abundances of ppERK and then calculated a sensitivity coefficient for each rate constant using Equation 1. We also varied each kinetic rate constant by -10% and calculated another sensitivity coefficient for each rate constant. The two sensitivity coefficients were then averaged to give a single sensitivity coefficient for every rate constant in each of the two models. As the Feedback Intact and Feedback Broken models share a large number of identical reactions, and therefore parameters, sensitivity coefficients can be directly compared to one another enabling the robustness of the models to be compared.

1.6: Non Steady-State Responses

We assessed the transient behavior of the system to further analyze the NFA characteristics of the ERK pathway. We stimulated the system and then, when ppERK abundances reached their maximum, we introduced the MEK inhibitor U0126, and monitored ppERK abundances over time to examine how the system responds to this disturbance. In theory, when the feedback loop is intact the system should recover from the disturbance caused by U0126 and ppERK abundances should increase reaching a new equilibrium. Whereas, when the feedback loop is broken, the system should fail to compensate for the disturbance caused by U0126 and ppERK abundances should not recover.

This investigation was performed as follows. First, we created a Feedback Intact model that contained no U0126 and no U0126 reactions. This model was simulated for 360 seconds (6 minutes) at which point ppERK abundances are at their maximum. Second, the final concentrations of all the species from this initial simulation were transferred to a new Feedback Intact model that did contain U0126 (10,000,000 molecules) and U0126 reactions. This means that the new U0126 model starts off from exactly the same position that the first non-U0126 model finished. Third, this U0126 model was then simulated for 3240 seconds (54 minutes) and the two simulation results were combined to give a 3600 second (1 hour) time course where U0126 was added at the peak of ERK activation (Fig.S6A). The same strategy was used for the Feedback Broken model, except that the concentration of BXB-ER (the input) was increased to 6,416 molecules for this simulation so that ppERK abundances for the two models were approximately the same at the point where U0126 was added Experimentally, these predictions were tested by adding U0126 at the peak of ERK activation (Fig. S6B). The results are consistent with the model predictions that the NFA will cause the system to recover at a higher activity

than the basal state, which is not possible without the negative feedback. The exact kinetics between the simulation and the experimental result are different, but this is not surprising because the effects of the inhibitor in the model are immediate, whereas in the experimental situation the inhibitor has to diffuse into the cell and accumulate to effective inhibitory concentrations.

1.7: The Effects of B-Raf

The Feedback Intact model included a single Raf isoform, Raf-1, and ignored B-Raf. We did not consider B-Raf initially because the COS1 cell line that we used does not have detectable amounts of B-Raf (14). However, most cells have both Raf-1 and B-Raf (15). In addition, B-Raf and Raf-1 heterodimerize (16-18), and oncogenic B-Raf mutants with low kinase activity were reported to need Raf-1 to efficiently activate ERK (16). The B-Raf/Raf-1 heterodimer has very high kinase activity towards MEK, although it is only formed at low stoichiometry (17). The formation of the B-Raf/Raf-1 heterodimer is mitogenic and induced by active Ras (16-18). The lifetime of the dimer, but not its formation, is subjected to a negative feedback by ERK (17, 19). The kinase activity of B-Raf is not susceptible to negative feedback regulation by ERK (Fig. S8).

These data suggest that B-Raf does not participate in the NFA. However, Raf-1 and B-Raf compete with each other for activation by RasGTP. This competition could possibly interfere with the NFA properties because the abundances of active B-Raf could decrease due to increased competition from Raf-1 when the negative feedback loop is weakened after drug treatment. This would mean that the overall abundances of active Raf species remains relatively constant, whereas increasing abundances of active Raf are needed to display NFA behavior. Therefore, we created the B-Raf Feedback Intact model in which the Feedback Intact model was expanded to include B-Raf (table S3) and to investigate the effect of B-Raf on the system's ability to behave as a NFA and resist the effects of the MEK inhibitor U0126. The presence of B-Raf did not eliminate the NFA characteristic that allowed the system to resist the effects of U0126 and to maintain relatively high abundances of ppERK over a broad range of U1026 concentrations (fig. M3), similar to the simulations of the Feedback Intact model (Fig. 3C). The simulations also showed that the abundances of active B-Raf remained relatively stable as the concentration of U0126 increased, whereas the abundances of active Raf-1 increased due to a weakening of the negative feedback loop from ERK to Raf-1 (fig. M4). Furthermore, assigning distinct phosphatases to Raf-1 and B-Raf to eliminate competition for deactivation had little effect (fig. M5). Therefore, these results suggest that B-Raf does not change the NFA characteristics of the ERK cascade and does not interfere with the system's ability to resist inhibition by U0126. A table of reactions, species, and kinetic parameters for the B-Raf Feedback Intact model is presented in the Model_B-Raf (table S3).

1.8: Computational Tools

We used Gepasi (20) (www.gepasi.org) as the computational tool for model construction, simulation, and analysis. We used the SimBiology toolbox of Matlab

() to double-check the simulation results obtained from Gepasi.
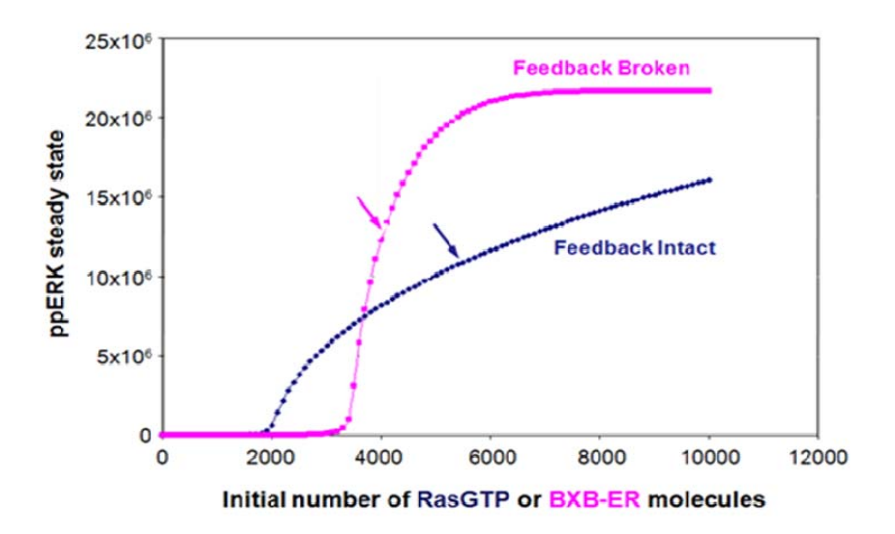
Section 1 figures M1-M5

Fig. M1. ERK-PP input/output response curves of the Feedback Intact and Feedback Broken models. The x-axis represents the input level which corresponds to initial BXB-ER molecules for the Feedback Broken model and initial RasGTP molecules for the Feedback Intact model; the y-axis represents total steady state [ERK-PP]. For each model, an arrow points to the input level that was selected and used for further investigations of the effects of the MEK inhibitor U0126 and for sensitivity analyses. The two arrows are not located at exactly the same point on the input x-axis because the input levels were selected based on normalisation at the level of active Raf whereas the x-axis corresponds to two different inputs (RasGTP & BXB-ER). However, both arrows are still in the centre of their corresponding response curves which means the two models are in a comparable state.
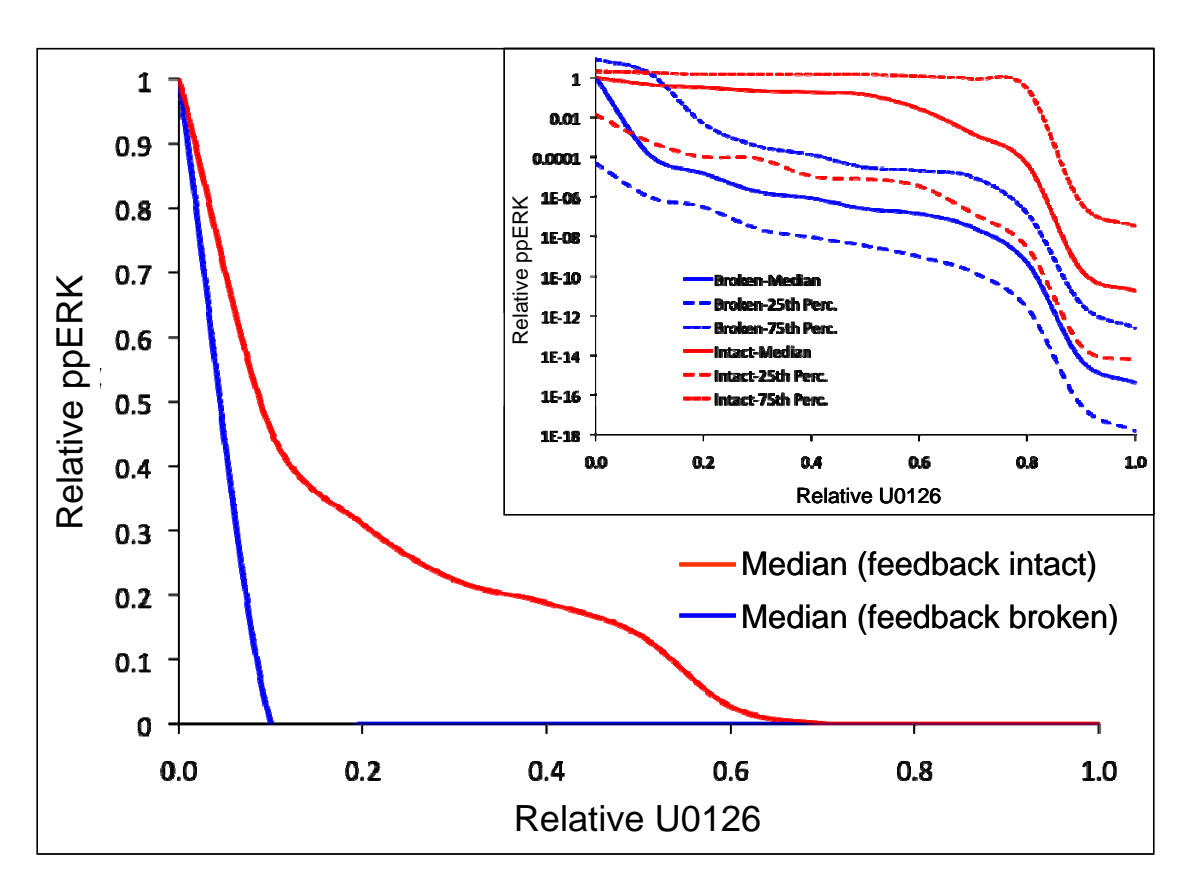
Fig. M2. Effects of parameter variations in the Feedback Broken and Feedback Intact models. *Parameters spanning +/- 1 order of magnitude from the nominal value were sampled in simulations with the various concentrations of U1026 as described in section 1.3. The medians of steady-state ppERK concentrations are plotted. The inset shows the median of the steady-state ppERK abundances along with the 25th and 75th percentiles. Note that the inset y-axis is on a log scale to assure that all curves are visible on the plot.*
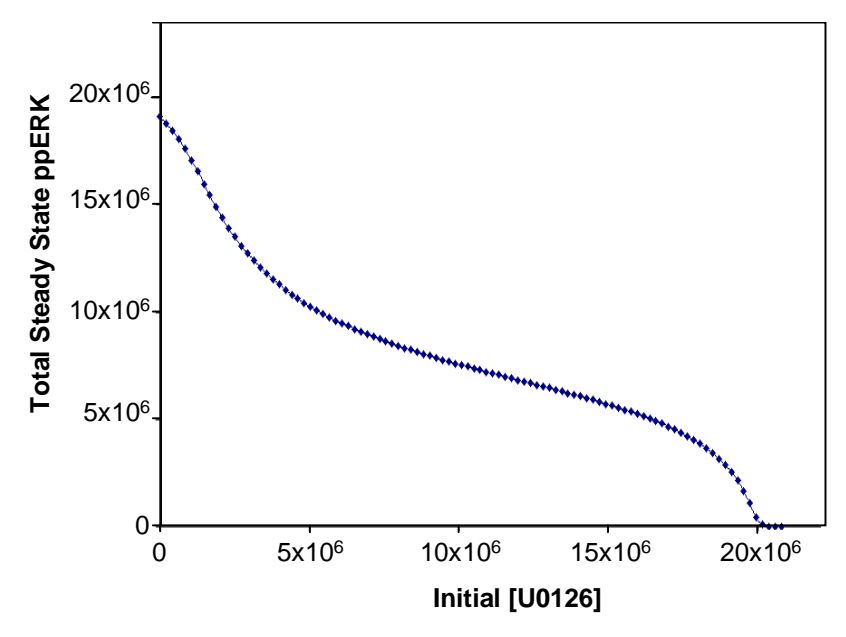
***Fig. M3. ppERK response of the B-Raf Feedback Intact model to an increasing initial
concentration of U0126.*** *This graph displays the steady-state concentration of total
ppERK (y-axis) after different initial concentrations of U0126 (x-axis) given as number of
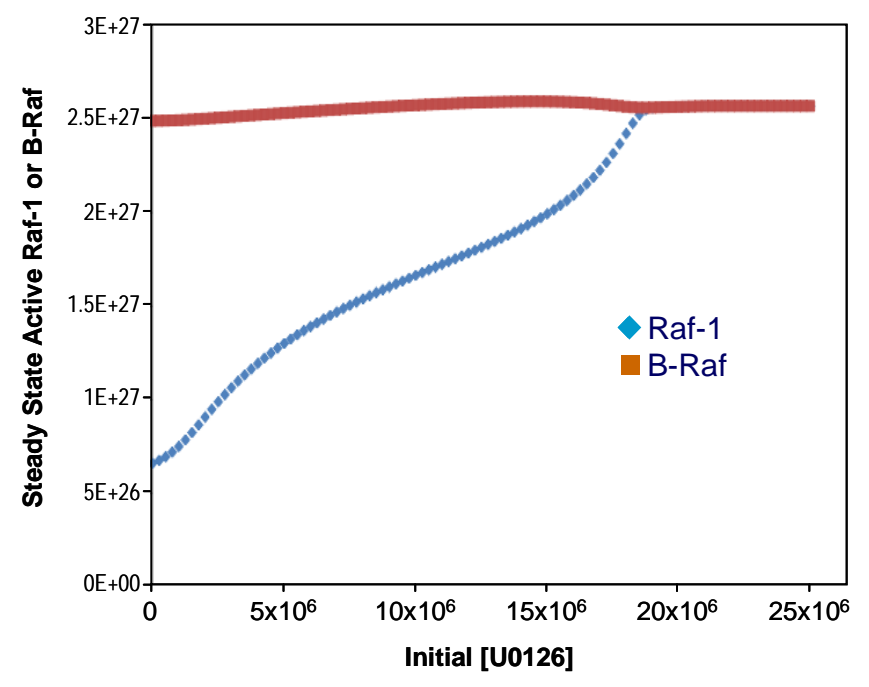molecules for the B-Raf Feedback Intact model.*

***Fig. M4. Active Raf-1 and B-Raf steady-state response to an increasing initial
concentration of U0126.*** *This graph displays the steady-state concentration of total
active Raf-1 or B-Raf (y-axis) after different initial concentrations of U0126 (x-axis) for
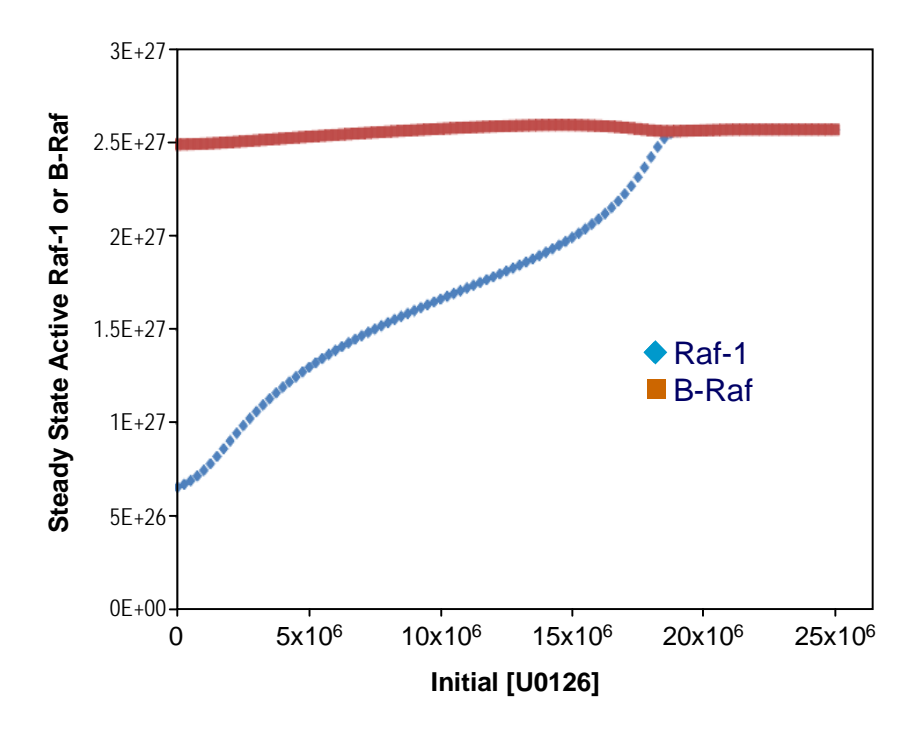the B-Raf Feedback Intact model.*

Fig. M5. Active Raf-1 and B-Raf steady-state response to an increasing initial concentration of U0126 when Raf-1 and B-Raf are deactivated by different phosphatises. *This graph displays the steady-state concentration of total active Raf-1 or B-Raf (y-axis) after different initial concentrations of U0126 (x-axis) for the B-Raf Feedback Intact model when separate phosphatases of equal abundance deactivate Raf-1 and B-Raf.*

Section 2. Model Parameters

The parameters for each model are presented in a single Excel file with an individual worksheet for table S1-3 of model parameters. The parameters include the forward and reverse rate constants, the rate number assigned to each rate constant, the units of the rate constants, and the starting amounts for each of the molecules, along with the sources upon which the parameters are based.

Table S1. Model_Intact in the Excel file corresponds to the Feedback Intact model.
Table S2. Model_Broken in the Excel file corresponds to the Feedback Broken model.
Table S3. Model_B-Raf in the Excel file corresponds to the Feedback Intact model in which the Feedback Intact model has been expanded to include B-Raf.

Section. 3. SBML Files of the Models
Systems Biology Markup Language (SBML; www.sbml.org) files of the models are provided.

References

1. B. Schoeberl, C. Eichler-Jonsson, E. D. Gilles, G. Muller, Computational modeling of the dynamics of the MAP kinase cascade activated by surface and internalized EGF receptors. *Nat Biotechnol* **20**, 370 (2002).
2. M. K. Dougherty, J. Muller, D. A. Ritt, M. Zhou, X. Z. Zhou, T. D. Copeland, T. P. Conrads, T. D. Veenstra, K. P. Lu, D. K. Morrison, Regulation of Raf-1 by direct feedback phosphorylation. *Mol Cell* **17**, 215 (2005).
3. A. S. Dhillon, W. Kolch, Untying the regulation of the Raf-1 kinase. *Arch Biochem Biophys* **404**, 3 (2002).
4. W. Kolch, Coordinating ERK/MAPK signalling through scaffolds and inhibitors. *Nat Rev Mol Cell Biol* **6**, 827 (2005).
5. C. Wellbrock, M. Karasarides, R. Marais, The RAF proteins take centre stage. *Nat Rev Mol Cell Biol* **5**, 875 (2004).
6. J. Urosevic, E. Y. Sum, V. Moneo, M. Drosten, A. Dhawahir, M. Becerra, A. Carnero, M. Barbacid, Using cells devoid of RAS proteins as tools for drug discovery. *Mol Carcinog* **48**, 1038 (2009).
7. M. F. Favata, K. Y. Horiuchi, E. J. Manos, A. J. Daulerio, D. A. Stradley, W. S. Feeser, D. E. Van Dyk, W. J. Pitts, R. A. Earl, F. Hobbs, R. A. Copeland, R. L. Magolda, P. A. Scherle, J. M. Trzaskos, Identification of a novel inhibitor of mitogen-activated protein kinase kinase. *J Biol Chem* **273**, 18623 (1998).
8. W. S. VanScyoc, G. A. Holdgate, J. E. Sullivan, W. H. Ward, Enzyme kinetics and binding studies on inhibitors of MEK protein kinase. *Biochemistry* **47**, 5017 (2008).
9. J. F. Ohren, H. Chen, A. Pavlovsky, C. Whitehead, E. Zhang, P. Kuffa, C. Yan, P. McConnell, C. Spessard, C. Banotai, W. T. Mueller, A. Delaney, C. Omer, J. Sebolt-Leopold, D. T. Dudley, I. K. Leung, C. Flamme, J. Warmus, M. Kaufman, S. Barrett, H. Tecle, C. A. Hasemann, Structures of human MAP kinase kinase 1 (MEK1) and MEK2 describe novel noncompetitive kinase inhibition. *Nat Struct Mol Biol* **11**, 1192 (2004).
10. M. L. Samuels, M. J. Weber, J. M. Bishop, M. McMahon, Conditional transformation of cells and rapid activation of the mitogen-activated protein kinase cascade by an estradiol-dependent human raf-1 protein kinase. *Mol Cell Biol* **13**, 6241 (1993).
11. J. Lovric, S. Dammeier, A. Kieser, H. Mischak, W. Kolch, Activated raf induces the hyperphosphorylation of stathmin and the reorganization of the microtubule network. *J Biol Chem* **273**, 22848 (1998).

12. S. Cockerill, C. Stubberfield, J. Stables, M. Carter, S. Guntrip, K. Smith, S. McKeown, R. Shaw, P. Topley, L. Thomsen, K. Affleck, A. Jowett, D. Hayes, M. Willson, P. Woollard, D. Spalding, Indazolylamino quinazolines and pyridopyrimidines as inhibitors of the EGFr and C-erbB-2. *Bioorg Med Chem Lett* **11**, 1401 (2001).

13. H. Kacser, J. A. Burns, The control of flux. *Symp Soc Exp Biol* **27**, 65 (1973).

14. E. M. Weissinger, G. Eissner, C. Grammer, S. Fackler, B. Haefner, L. S. Yoon, K. S. Lu, A. Bazarov, J. M. Sedivy, H. Mischak, W. Kolch, Inhibition of the Raf-1 kinase by cyclic AMP agonists causes apoptosis of v-abl-transformed cells. *Mol Cell Biol* **17**, 3229 (1997).

15. G. Galabova-Kovacs, A. Kolbus, D. Matzen, K. Meissl, D. Piazzolla, C. Rubiolo, K. Steinitz, M. Baccarini, ERK and beyond: insights from B-Raf and Raf-1 conditional knockouts. *Cell Cycle* **5**, 1514 (2006).

16. M. J. Garnett, S. Rana, H. Paterson, D. Barford, R. Marais, Wild-type and mutant B-RAF activate C-RAF through distinct mechanisms involving heterodimerization. *Mol Cell* **20**, 963 (2005).

17. L. K. Rushworth, A. D. Hindley, E. O'Neill, W. Kolch, Regulation and role of Raf-1/B-Raf heterodimerization. *Mol Cell Biol* **26**, 2262 (2006).

18. C. K. Weber, J. R. Slupsky, H. A. Kalmes, U. R. Rapp, Active Ras induces heterodimerization of cRaf and BRaf. *Cancer Res* **61**, 3595 (2001).

19. T. Brummer, H. Naegele, M. Reth, Y. Misawa, Identification of novel ERK-mediated feedback phosphorylation sites at the C-terminus of B-Raf. *Oncogene* **22**, 8823 (2003).

20. P. Mendes, GEPASI: a software package for modelling the dynamics, steady states and control of biochemical and other systems. *Comput Appl Biosci* **9**, 563 (1993).
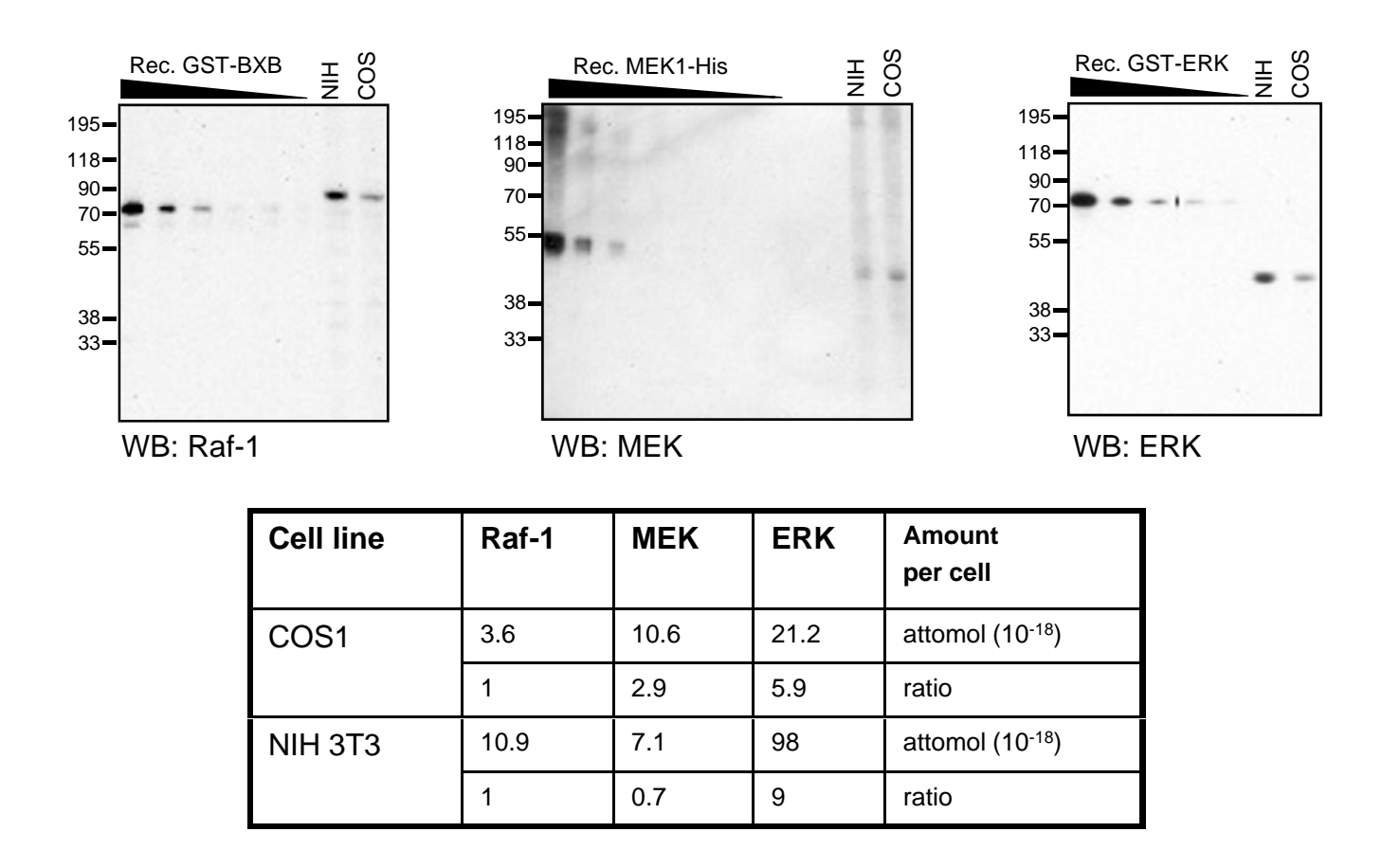
WB: Raf-1

Rec. GST-BXB   NIH   COS

195—
118—
90—
70—
55—
38—
33—

WB: MEK

Rec. MEK1-His   NIH   COS

195—
118—
90—
70—
55—
38—
33—

WB: ERK

Rec. GST-ERK   NIH   COS

195—
118—
90—
70—
55—
38—
33—

Cell line	Raf-1	MEK	ERK	Amount per cell
COS1	3.6	10.6	21.2	attomol (10^{-18})
	1	2.9	5.9	ratio
NIH 3T3	10.9	7.1	98	attomol (10^{-18})
	1	0.7	9	ratio

Fig. S1. Absolute concentrations of Raf-1, MEK, and ERK in COS1 and NIH 3T3 cells. Recombinant proteins representing the Raf-1 kinase domain (GST-BXB), MEK1 (MEK1-His) and ERK2 (GST-ERK) were expressed in E.coli and purified to >80% homogeneity as judged by Coomassie staining. These recombinant protein were used as standards to determine the concentrations of the respective proteins in lysates of NIH/3T3 and COS1 cells. To estimate molar concentrations per cell, an average cell volume of 5pL was used.
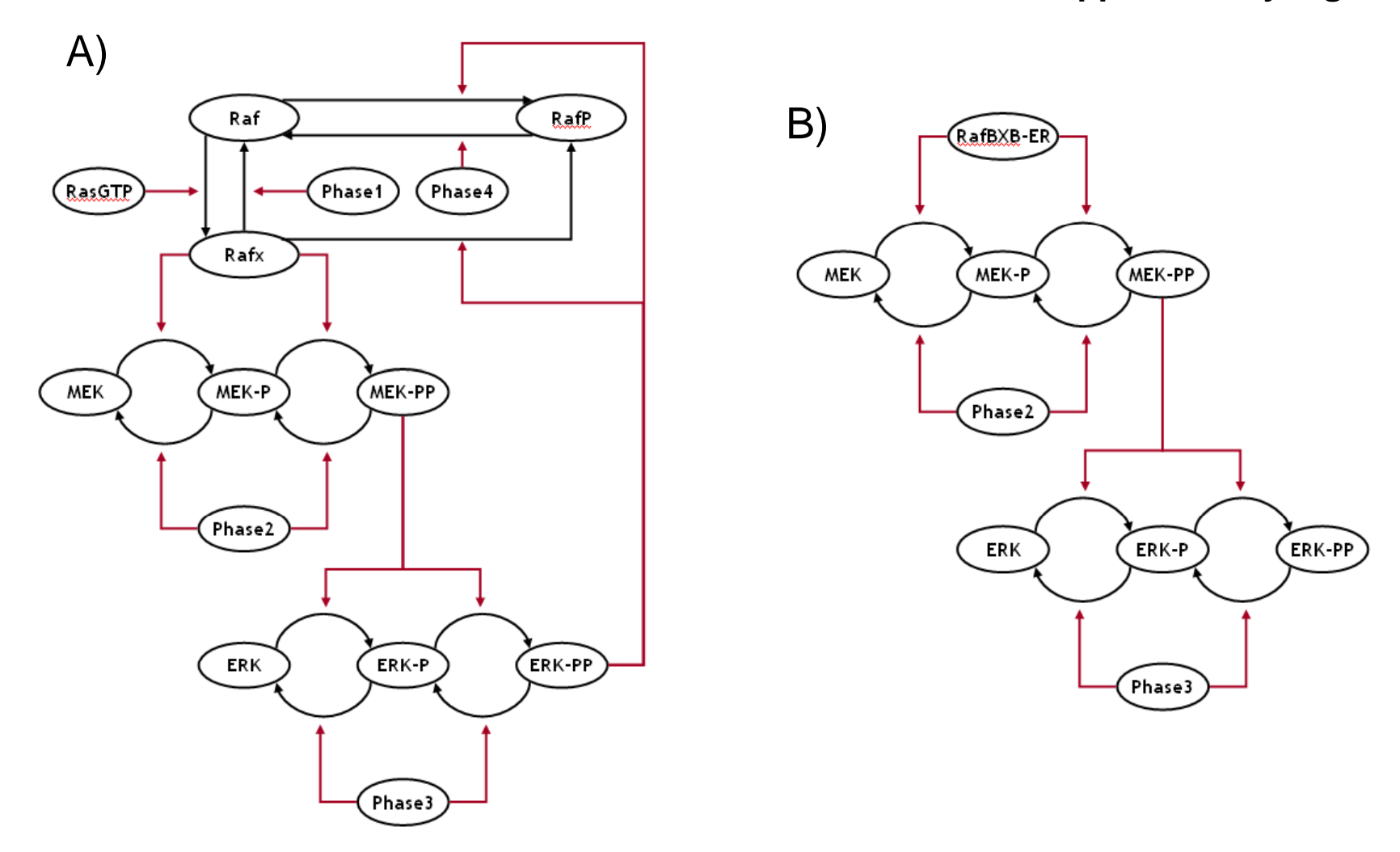
Fig. S2. Schematic topologies of the models used. (A) The Feedback Intact model starts at the level of RasGTP and ends at the level of ERK. It includes a negative feedback loop from activated ERK to both active and inactive Raf. Rafx, activated Raf; RafP, Raf deactivated by ERK feedback phosphorylation; Phase, phosphatase; MEK-P, ERK-P and MEK-PP, ERK-PP, single and double phosphorylated MEK and ERK, respectively. (B) The Feedback Broken model starts at the level of RafBXB-ER, ends at the level of ERK and does not include a negative feedback loop.
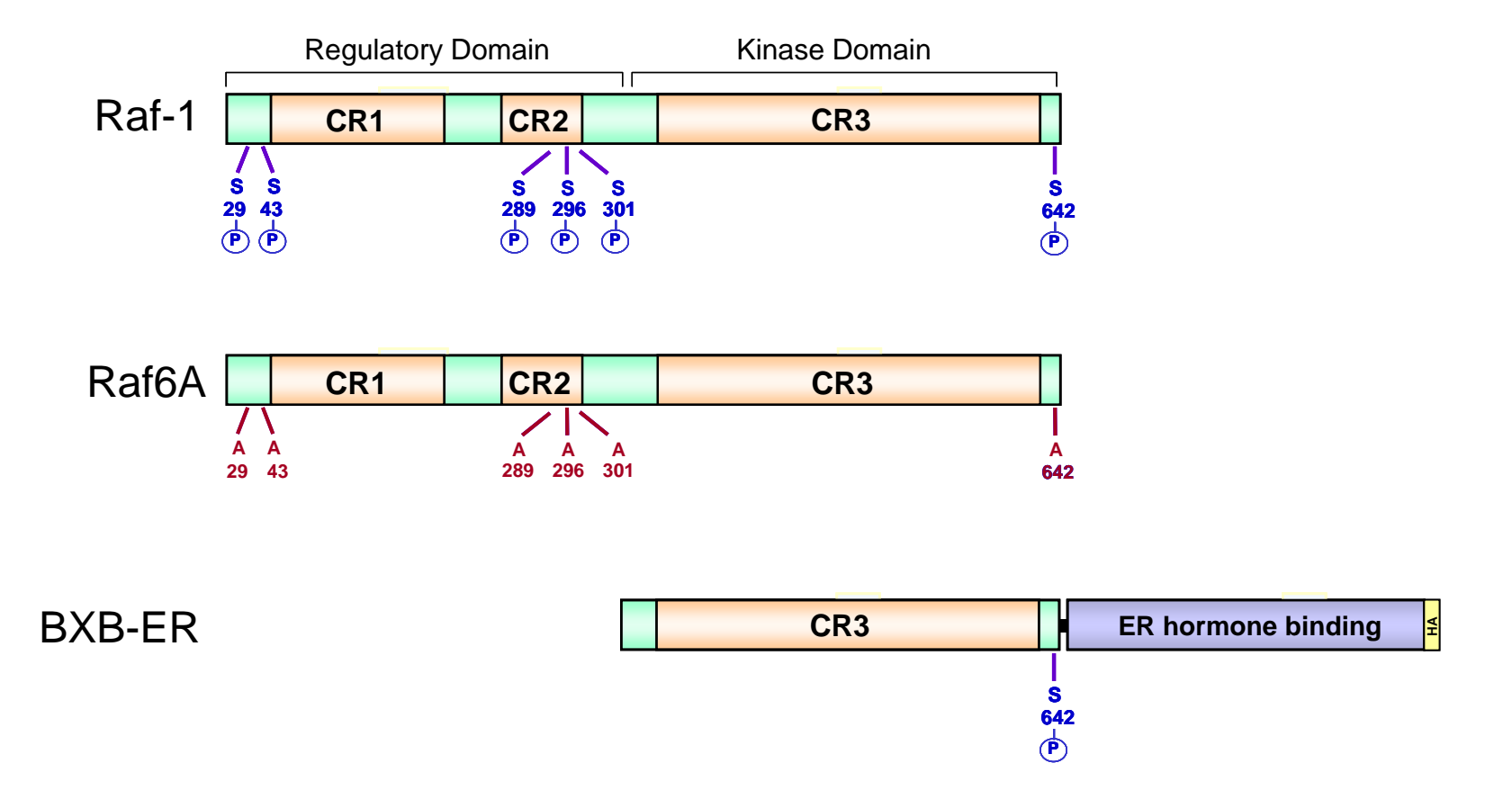
Fig. S3. Schematic of Raf-1 and the Raf-1 mutants used to probe the NFA hypothesis.
Inhibitory ERK phosphorylation sites as mapped by Dougherty et al. Mol Cell 17, 215-224 (2005) are indicated. In the Raf-1 6A mutant (a kind gift from D. Morrison) these serines are replaced by alanines. BXB-ER contains the Raf-1 kinase domain fused to the hormone binding domain of the estrogen receptor (ER). For ease of detection and isolation an HA-tag was added to the C-terminus (Lovric et al., J Biol Chem. 273, 22848-22855, 1998). CR; conserved region.

Fig. S4. Expression of Flag-tagged Raf-1 and the Raf6A mutant were tested by Western blotting with a Raf-1 specific antibody. ERK1/2 expression was used as loading control.
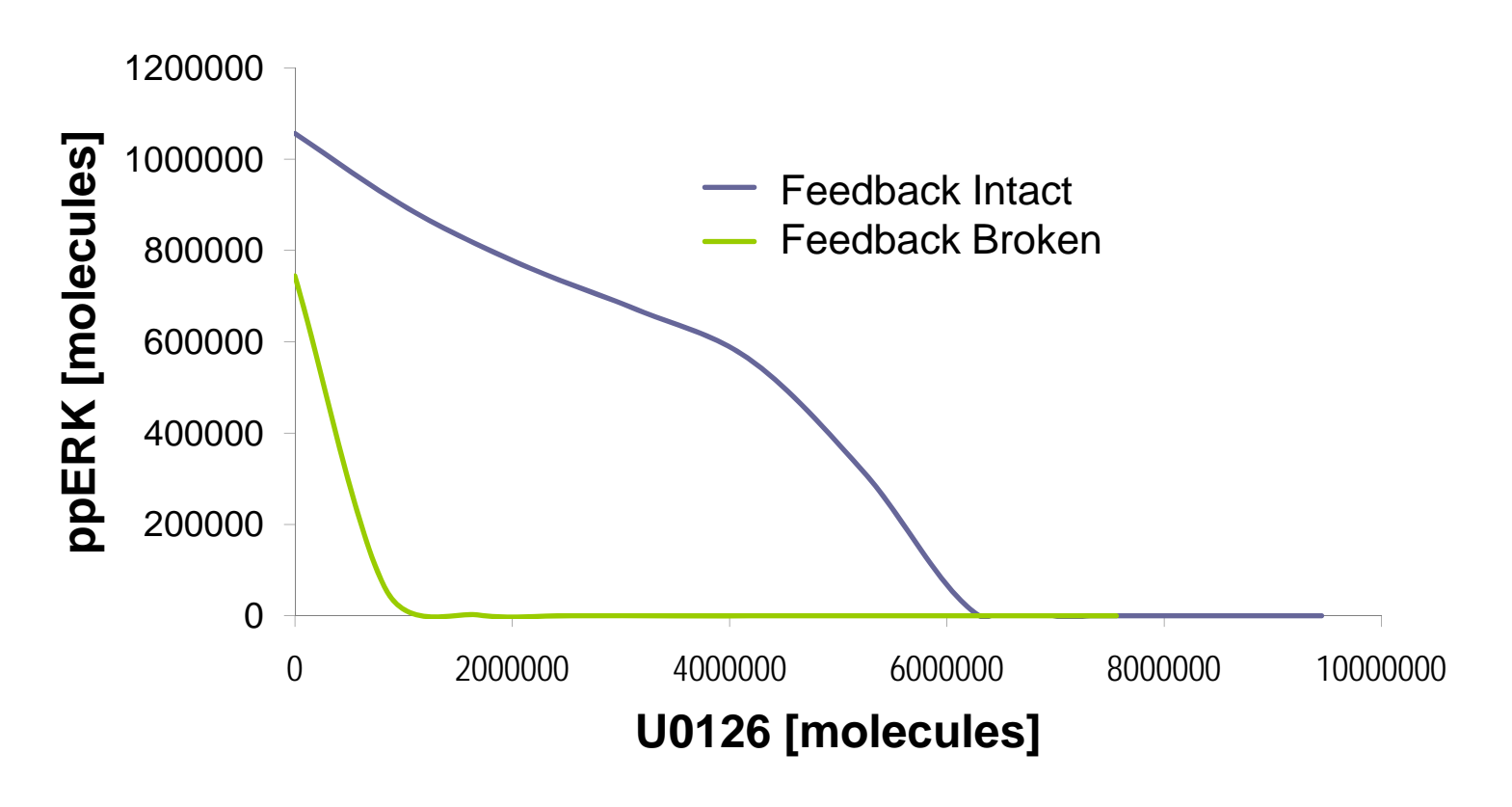
Fig. S5. The effects of U0126 on steady-state ppERK abundance with protein concentrations of COS1 cells. Total protein concentrations as determined in fig. S1 for COS1 cells were taken as (in molecules/cell): Raf-1 (2 million), MEK (6 million), ERK (12 million). For the Feedback Intact model, the RasGTP input was set to 2500 molecules/cell, whereas for the Feedback Broken model, the active Raf input was set to 4800 molecules/cell.
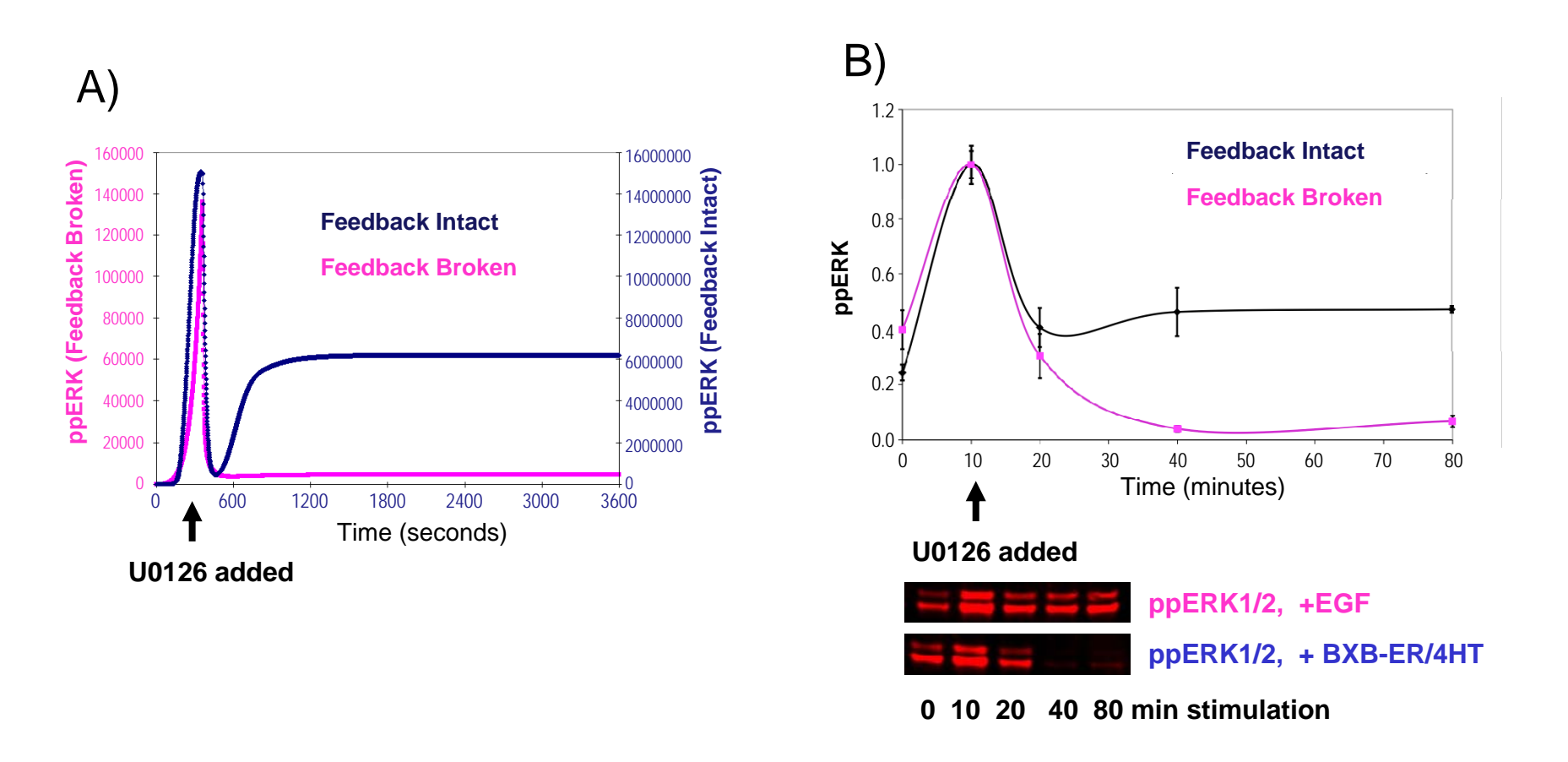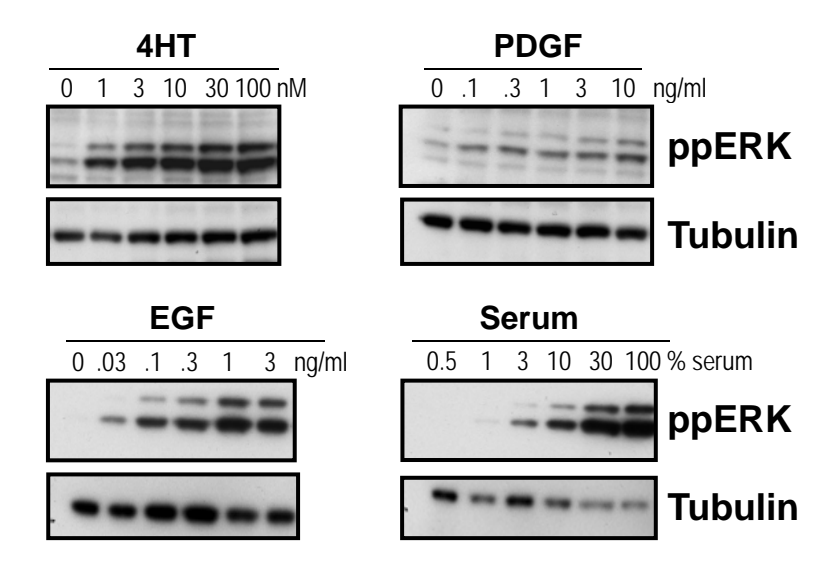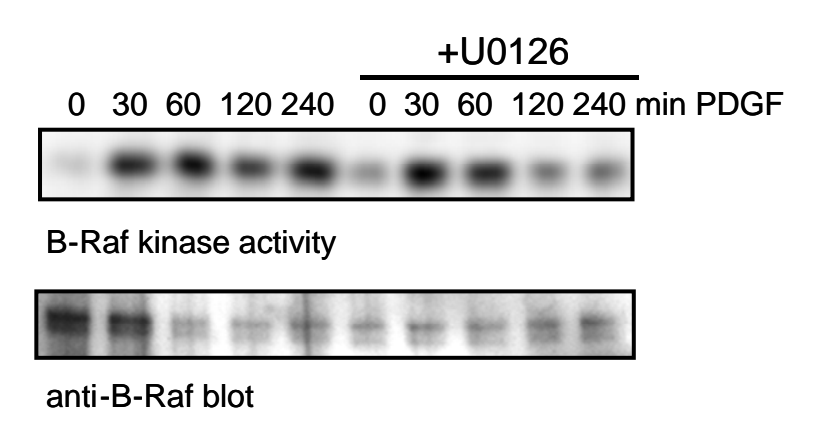
Fig. S6. The NFA effect also stabilizes non-steady-state dynamic systems.
(A) Simulation of adding U0126 at the peak of ERK activation. **(B)** Experimental results of adding U0126 at the peak of ERK activation. A stable BXB-ER COS1 cell line was stimulated with EGF or 4-Hydroxy-tamoxifen (4HT). In both cases, 1 μM of U0126 was added 10 minutes after treatment with EGF or 4HT. ERK activity was measured by LICOR.

Fig. S7. Dose-dependent ERK activation by different stimuli. NIH/3T3 cells stably expressing BXB-ER(*31*) were stimulated with increasing amounts of 4-hydroxy-tamoxifen (4HT), platelet derived growth factor (PDGF), epidermal growth factor (EGF), or foetal calf serum (serum). ERK phosphorylation (ppERK) was determined by Western blotting. Tubulin was used loading control.

+U0126

0 30 60 120 240   0 30 60 120 240 min PDGF

B-Raf kinase activity

anti-B-Raf blot

Fig. S8. B-Raf kinase activity is not feedback-inhibited by ERK. Endogenous B-Raf was immunoprecipitated from cells treated with 50ng/ml PDGF for the indicated time points. B-Raf kinase activity was measured as described (Rushworth et al. Mol Cell Biol 26, 2262-2272 2006) using GST-MEK as substrate.